Comparison of the optoelectronic properties of oxidized and non-oxidized substituted benzothiophene. Application to solution air-processed OLEDs

Khaled Youssef, Akpeko Gasonoo, Charles Cougnon, Matthieu Loumaigne, Hayley Melville, Lionel Sanguinet, Gregory Welch, Frédéric Gohier

Comparison of the optoelectronic properties of oxidized and non-oxidized substituted benzothiophene. Application to solution air-processed OLEDs.

Khaled Youssef,[a] Akpeko Gasonoo,[b] Charles Cougnon, [a] Hayley Melville, [a] Lionel Sanguinet, [a] Gregory C. Welch,[b] et Frédéric Gohier[a*]

[a.] *Univ Angers, CNRS, MOLTECH-Anjou, SFR MATRIX, F-49000 Angers, France.*
[b.] *Department of Chemistry, University of Calgary, Calgary, Alberta T2N 1N4, Canada*
Email :frederic.gohier@univ-angers.fr

Benzothiophenes and benzothiophene S,S-dioxide substituted with triphenylamines at positions 3,5,6 and 2,4,7 were synthesized in 2 or 3 steps and exhibited emission properties in both solution and solid states. OLED devices were fabricated through air process spin-coating, except for the silver cathode which was evaporated under vacuum. A flexible device based on 2,4,7-trimethoxyphenylbenzothiophene S,S-dioxide was successfully printed on PET on large surface .

The first OLEDs by Tang and Van Slike[1] were a simple sandwich of an emissive layer between two electrodes with more than decent performance. Since this discovery, this technology has rapidly developed[2, 3] and has even been commercialized in television displays, phones, computers, etc. They have the advantage of not being too power-consuming and having a color contrast that makes them difficult to compete within this field. Additionally, the ability to display on flexible materials allows them to be integrated into various devices, particularly in the medical field. [4-7] OLED device fabrication is achieved through vacuum evaporation, allowing for homogeneous layers formation. It is now challenged by wet deposition processes[8] that enable the production of larger format devices. Thus, the first layers, hole transporting Layers (HTL) and emissive layer, are deposited by wet deposition, and the remainder by evaporation. Few examples in the literature also present the wet deposition of the electron transporting layer (ETL). The first example of wet deposition of all the layers between the electrodes was achieved by spin casting on a glass support in a controlled atmosphere. In this way, an OLED was produced with the deposition of PEDOT:PSS (HIL, hole-injection layer), polyfluorene TFB (HTL), the emitter layer and TPBI or BPOPB (ETL). [9] The electrodes can also be deposited by printing, and the performance achieved equals that of OLEDs produced by evaporation.[10] Other examples, Welch et al[11] deposited 4 successive layers via slot-die coating on PET coated with ITO using PEDOT-PSS as HIL, PVK as HTL, an emissive layer, and then ZnO as ETL. In another paper, they demonstrate the ability to substitute ZnO with PFN to manufacture large-area OLEDs.[12] The specifications are more complex because each layer requires a solvent that will not redissolve the layer upon which it is deposited. The need to work with new emissive products with the right solvation properties is an avenue to explore. In this context, we became interested in benzothiophene SS-dioxide, since a number of articles mention quite interesting emission starting from benzothiophene. Tang and coll[13, 14] have shown that BTO substituted in positions 2 and 3 with aromatic groups such as Ph, substituted Ph, TPA (triphenylamine) and thiophene derivatives systematically led to emission in the solid state. Emission in solution was only possible if the substituents were bulky enough to prevent intramolecular rotation of these groups. Liou and coll[15] demonstrated that with only one substituted position, specifically a TPA in position 3, they also observed emission utilized in electrochromic cells. Position 2 could also be easily functionalized with TPAs, carbazoles[16] or vinyl derivatives[17] on the BTO, resulting in emission in solution and in the solid state.

In this article, benzothiophenes (BT) and oxidized benzothiophenes (BTO) were synthesized with bromine substituents at positions 2,4,7 and 3,5,6, which are challenging to functionalize using conventional methods in such few steps. Couplings with triphenylamine resulted in five different compounds, whose opto-electronic properties were compared. The position of TPA on these motifs somewhat influenced absorption and emission properties, and the oxidized benzothiophene exhibited changes in HOMO/LUMO levels, impacting absorption, emission, and electrochemical properties. The application of oxidized compounds in OLED devices produced by spin coating or slot-die printing for all layers except the cathode has also been achieved. Finally, an example of a flexible OLED device on PET was produced.

Scheme 1: Preparation of 3,5,6 and 2,4,7 tribrominated benzothiophenes

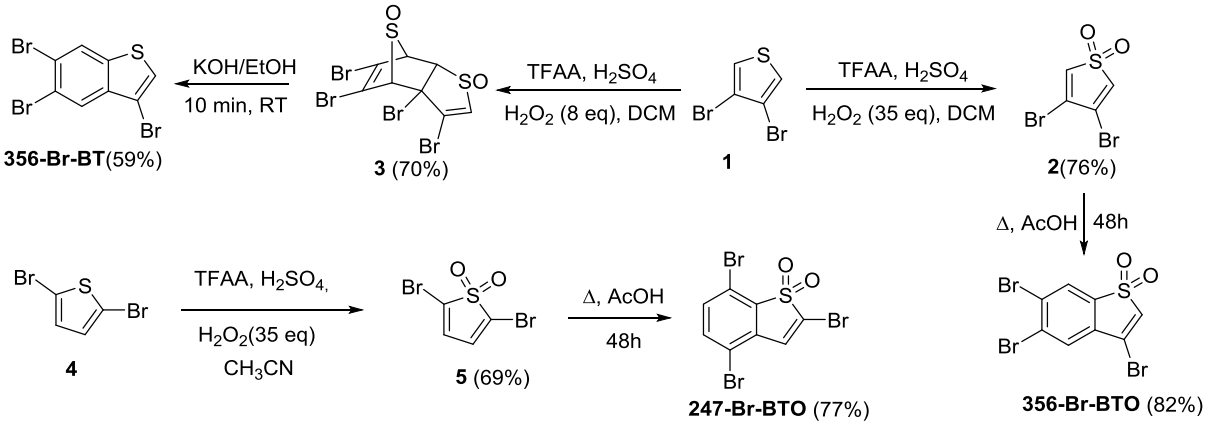

The oxidation of thiophene leads to thiophene S-oxide and then to S,S-dioxide under oxidative conditions such as mCPBA or H_2O_2. However, isolating these species is not always easy as they can undergo further transformations; the diene/dienophile aspect becomes significantly pronounced with the loss of aromaticity. Nakayama[18] and Thieman[19] have made substantial contributions to these studies. Oxidized thiophene can be readily trapped by dienophiles such as quinone,[20] and the use of *in situ* dienophile is sometimes necessary, otherwise dimerization is observed.[21]

In our work, we demonstrated that the oxidation of 2,5-dibromo and 3,4-dibromothiophene could lead to brominated benzothiophenes at positions 3,5,6 (this isomer is called 356) and 2,4,7, (this isomer is called 247) whether oxidized or not, in 2 or 3 steps (scheme 1).[22] For the regioisomer 3,5,6, oxidation conditions favor the formation of the sulfone, mainly using a large excess of H_2O_2. The sulfone is stable at room temperature. If this reagent is used in too small amount, the intermediate sulfoxide accumulates and dimerizes due to its high instability. The corresponding benzothiophene forms in a few minutes in the presence of base with a yield of 59%. It appears that the sulfoxide is eliminated concomitantly with bromine, and the reduction of the second sulfoxide is achieved *in situ*. There are a few examples in the literature similar to our case without a clear idea about the mechanism. The treatment of diarylsulfoxide with a strong base allows for the formation of benzothiophenes; however, the method for reducing the sulfoxide is not specified. In another study, the use of a strong base with CuCl is mentioned to obtain reduced benzothiophenes, but this time starting from diarylsulfones. [23] For other substrates, such as pyridine N-oxides, sulfur dioxide has previously been utilized as a reductive agent.[24]

The sulfone dimerizes when the medium is heated to 170°C for 2 days, leading to the formation of benzothiophene S,S-dioxide. The regioisomer 2,4,7 is obtained through the same pathway. Since positions 2 and 5 are substituted, obtaining benzothiophene via sulfoxide is not possible. Attempts to reduce the sulfone to the sulfide did not yield benzothiophene; instead, a mixture of complex

products, which we have not identified, was formed. Subsequently, Suzuki-type couplings were carried out, either with the boronic acid of TPA or TPA substituted with methoxys. Compounds resulting from the three couplings were isolated with yields of up to 85%.

Scheme 2 : Syntheses of substituted **BT** and **BTO** by Suzuki couplings

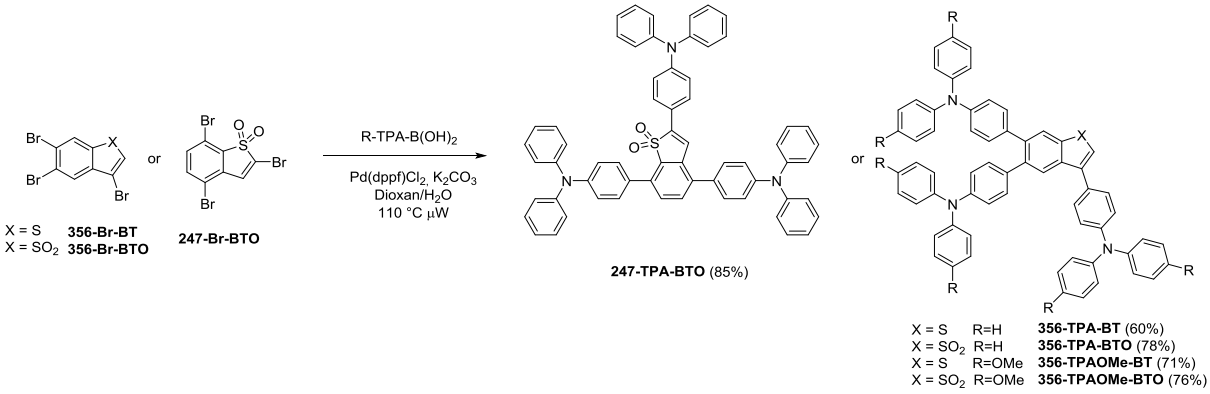

From these five products, we examined the produced effect on the opto-electronic properties between a benzothiophene (BT) and a benzothiophene S,S-dioxide (BTO), and between functionalization by TPAs at positions 3,5,6 and 2,4,7. The absorbance spectra (figure 1) in DCM resulted in three distinct behaviors. The non-oxidized compound with simple TPAs exhibits a maximum absorption at 291 nm and is colorless with an onset absorbance not exceeding 348 nm. The addition of MeO to TPAs causes a significant destabilization of HOMO levels, and the onset absorbance shifts by 34 nm towards higher wavelength. The oxidation of BT leads to the loss of aromaticity, and the dienic character is further strengthened, resulting in the emergence of a charge transfer band in the visible range (392 nm for **356-TPA-BTO** and 404 nm for **356-TPAOMe-BTO**). What was somewhat less predictable is the appearance of a second charge transfer band for the isomer 2,4,7 (**247-TPA-BTO**) at 433 nm.

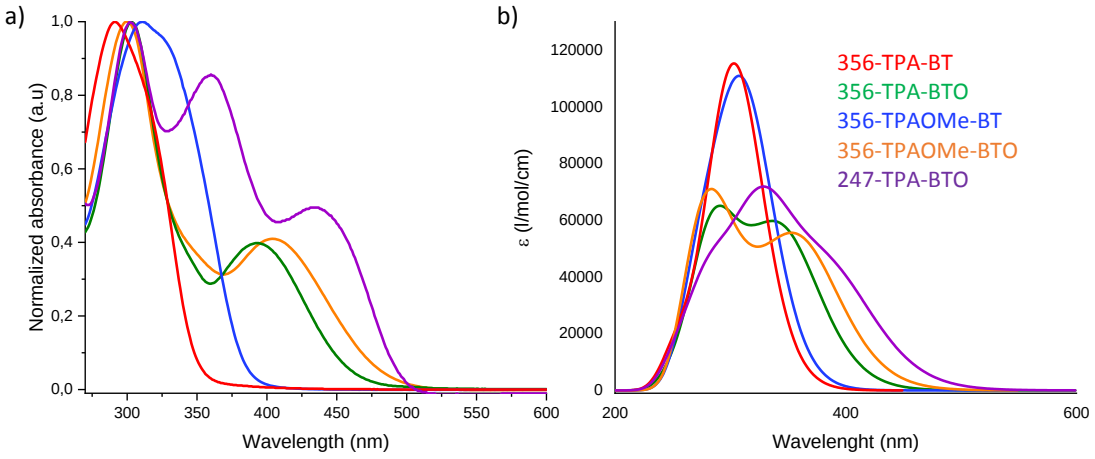

Figure 1 : UV-vis spectra a) experimental spectra in DCM solution at 10^{-5} mol/l and b) theoretical spectra in DCM with TD/M062X/6.311G+(d) IEFPCM

Intrigued by this change in structuring, theoretical calculations were carried out using the base TD/M062X/6.311G(d). All the results are gathered in the SI. On figure 2, the main electronic transitions partly responsible for the structuring of the spectra are represented for the compounds **356-TPA-BT**, **356-TPA-BTO**, and **247-TPA-BTO**.The simulated absorption spectra after calculation

closely resemble the structuring of spectra obtained in DCM solution (see figure 1b). The non-oxidized compounds exhibit degenerate HOMO and HOMO-1 levels localized on the TPA and the LUMO level more concentrated on the benzothiophene core. This charge transfer band shifts towards longer wavelengths when the benzothiophene core is oxidized, stabilizing the LUMO level. Charge transfer occurs from the HOMO-1 and HOMO-2 levels localized on the 3 TPA to the LUMO localized on the benzothiophene S,S-dioxide. To explain the three-band structuring of the 2,4,7 isomer, one must consider the more stabilized LUMO+1 level compared to the 3,5,6 isomer. Two charge transfer bands can be described: one between the HOMO level (delocalized over the entire molecule) and the LUMO+1 level (localized more on the BTO phenyl), and the other involving the participation of the HOMO-1 and HOMO levels towards the LUMO level (localized on the BTO core).

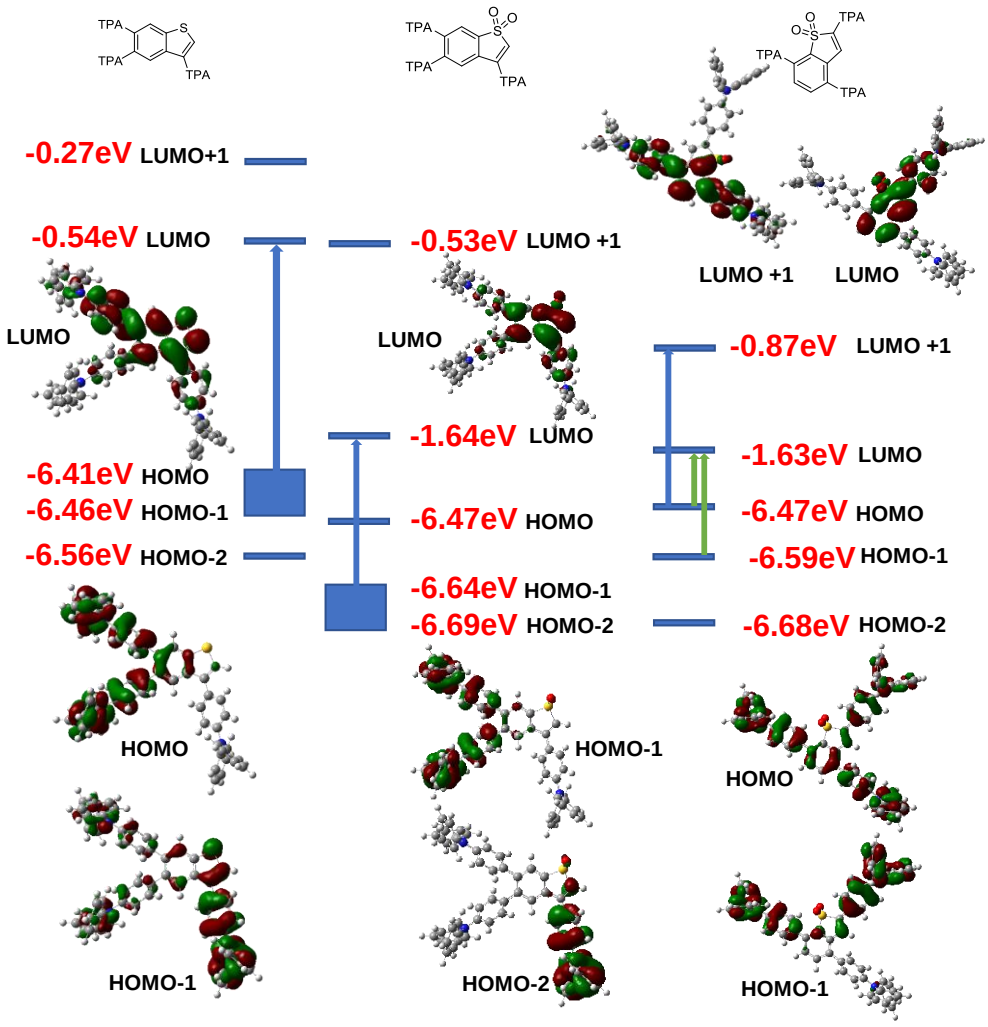

Figure 2: Representation of the main energy transitions observed for the compounds **356-TPA-BT**, **356-TPA-BTO**, and **247-TPA-BTO** determined by theoretical calculations using the MOX62/6.311G+(d) functional.

Table 1: Electro-optical properties of the studied compounds

Cpd	λmax (nm)	λonset (nm)	Gap[a]	E_{Ox} (V vs Fc)[b]	HOMO[c]	LUMO[d]
356-TPA-BTO	303, 392	455	2.73	0.58 (rev)	-5.53	-2.80
356-TPA-BT	291	348	3.57	0.54 (rev)	-5.50	-1.93

356-TPAOMe-BTO	300, 404	479	2.59	0.31 (rev) 0.89 (ir)	-5.33	-2.74
356-TPAOMe-BT	311	382	3.25	0.22 (rev) 0.85 (ir)	-5.25	-2.00
247-TPA-BTO	303, 360, 434	502	2.47	0.57 (rev)	-5.50	-3.03

[a] Determined from the onset of absorbance. [b] Determined in a cell with 3 electrodes (WE: Pt, CE:Ag wire, Ref: Ag/AgCl) with 0.1 M nBu_4NPF_6 as electrolyte in DCM. [c] Determined by PESA measurement. [d] LUMO = HOMO + gap.

Electrochemistry was performed on the various compounds in DCM using 0.1 M Bu_4NPF_6 as the supporting electrolyte. Each compound exhibits a reversible oxidation wave between 0.5V and 0.6V versus ferrocene, except for **356-TPAOMe-BT** and **356-TPAOMe-BTO**, which are more easily oxidized, likely due to the presence of methoxy groups. Moreover, these compounds show a second non-reversible oxidation wave. The latter was not observed for the other compounds within the studied potential window. HOMO level was determined by PESA. As expected, the LUMO levels of the BTO are stabilized compared to BT (-3.03, -2.80, -2.74 vs. 1.93 and -2.00) and the HOMO levels of the compounds with MeO as a substituent experience HOMO destabilization (-5.33, -5.25 vs. -5.50 and -5.53).

The emission spectra in solution and in the solid state were obtained for the five compounds. All of them exhibit dual emission properties except **for 356-TPAOMe-BTO**, which only emits in the solid state. For the latter, it has been demonstrated that when a solution of this compound in THF is enriched with water (see SI), emission is observed after the addition of 10% water, a phenomenon attributed to the aggregation of the compound in the solution. This emission then decreases with an increase in the water fraction. When the water fraction reaches 80%, a new band appears around 600 nm, emitting as observed in the solid state. Comparing with the literature, Tang et al.[13] described AIE properties on BTO substituted at positions 2 and 3 with aryls having low steric hindrance (4-F-Ph, 4MeO-Ph, 4-CF_3-Ph, etc.). They demonstrated that this phenomenon can transition to dual state emission (DSE) if the steric hindrance is increased, as in the case of triphenylamine (TPA) or orthotolyl. Non-radiative relaxation is then prevented, preventing any rotation of these groups in solution. Liou et al.[15] worked on BTO substituted in position 3 with TPA and TPAOMe. The compound with TPAOMe exhibits typical AIE properties, similar to the compound with TPA, which, however, emits slightly in solution without water. In our case, the emission in solid state is present, which can be easily explained by restricted mobility at the aggregate level, allowing radiative emissions. This emission proves to be more significant in solution. Wei, Gong, et al.[25] explain in an article on the TPA group that it is prone to DSE due to its twisted molecular conformation and molecular steric hindrance of phenyls.

Table 2: Maximum emission in solution (DCM, absorption<0.1) and solid state (powder) and corresponding quantum yields

Compound	λ_{exci} [nm]		λ_{em} [nm]		Φ [%][a]	
	Soln	Solid	Soln	Solid	Soln	Solid
356-TPA-BTO	390	370	589	540	54.9	36.8
356-TPA-BT	310	380	424	455	51.8	22.5
356-TPAOMe-BTO	405	370	/	588	0	21
356-TPAOMe-BT	310	370	465	470	79.8	24.3
247-TPA-BTO	430	370	551	557	59.1	39.8

[a] Determined with an integration sphere.

The coordinates of each compound were determined using online sci-sim software[26] and show that BTs emit in the blue (356-TPA-BT ✔ 0.16,0.15 ✔ ; 356-TPAOMe-BT ✘ 0.17, 0.25 ✘) and BTOs emit from

green to orange (356-TPA-BTO☎0.37,0.60☎; 356-TPAOMe-BTO⅄0.54, 0.45⅄; 247-TPA-BTO✦0.44, 0.54✦).

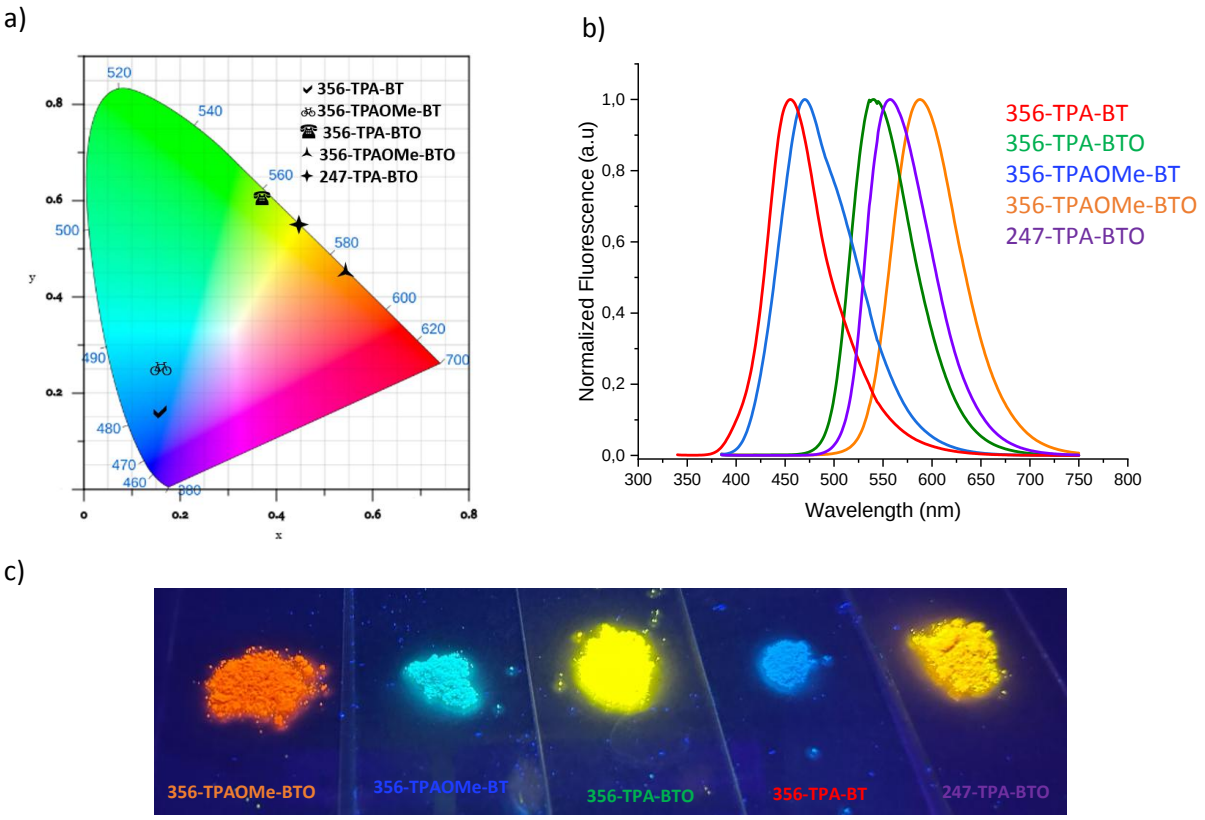

Figure 3: a) CIE chromaticity diagram 1931 determined from the emission spectra of the powder of the 5 compounds. b) Normalized Emission spectra recorded on powder of the 5 compounds. c) Pictures of the different compounds under 365 nm illumination.

The production processes of OLEDs are quite lengthy if one aims to move towards entirely printed OLEDs. We have decided to focus on BTO-based compounds and manufacture OLEDs entirely through spin coating on glass substrate on which a layer of ITO has already been deposited. The procedures for manufacturing OLEDs through evaporation are well-known; however, the printing of such devices becomes more complex as the created sandwich structure requires the deposition of a well-controlled layer. To achieve this, each layer must be deposited in a different solvent that does not solubilize the layer it comes into contact with. This orthogonal deposition reduces the number of candidates for printed OLED devices. Solubility and dissolution resistance studies have been conducted on various BTO compounds. As a result, **356-TPA-BTO** and **356-TPAOMe-BTO** are soluble in xylene and ethyl acetate, while **247-TPA-BTO** is only soluble in xylene, the chosen solvent for deposition on the PVK layer (not soluble in xylene). On the other hand, to deposit the electron transport layer (here PFN), BTO compounds must not be soluble in alcohols. The results presented in the table demonstrate adequate resistance to MeOH for the BTO compounds, the chosen solvent for this step. To verify this, the absorbance of the three BTO compounds deposited by spin-coating on a glass substrate was measured and compared to the absorbance of the same substrates after spin-coating with the solvent used for the deposition of the next layer (see SI).

Table 3: Solubility of BTO with various solvent

Compound	Solubility in[a]		Resistance (%) to dissolution with[b]		
	AcOEt	Xylene	MeOH	EtOH	BuOH
356-TPAOMe-BTO	good	good	88	72	82
356-TPA-BTO	good	good	51	49	0
247-TPA-BTO	X	good	62	77	73

[a] Dissolution at RT of 30 mg in 1 ml of solvent followed by visual check. [b] Ratio of absorbance on glass slice of washed compound over freshly deposited compound (see SI)

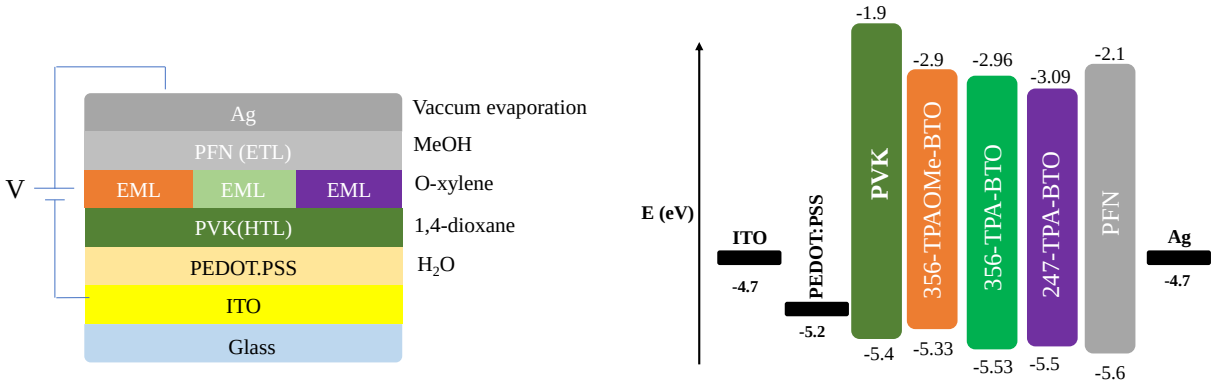

Figure 4: Representation of deposited OLED and corresponding HOMO-LUMO level

According to the schematic diagram shown in figure 4, PEDOT-PSS, a hole injection layer to facilitate hole injection, was deposited in solution in water. Polyvinylcarbazole (PVK), the hole-transporting layer, was deposited in dioxane. The emitter layer was then deposited in xylene, followed by the PFN (Electron transporting layer, ETL) in methanol, and finally the last silver electrode was the only layer to be evaporated to form the OLED device. The HIL, HTL and ETL layers have already been the object of significant attention for the preparation of printed OLEDs.[27] The devices were then tested. The results are presented in Fig. 5, and the characteristic data of the OLEDs which have performed the best are grouped in Table 4.

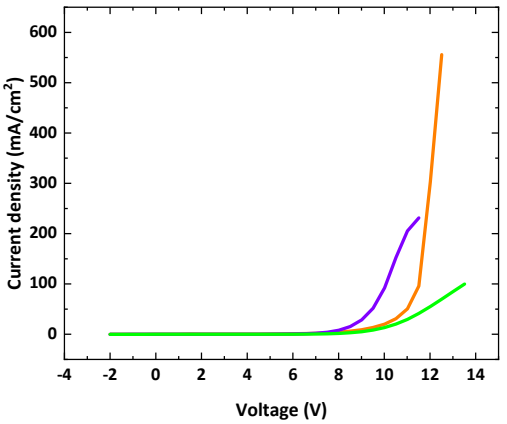

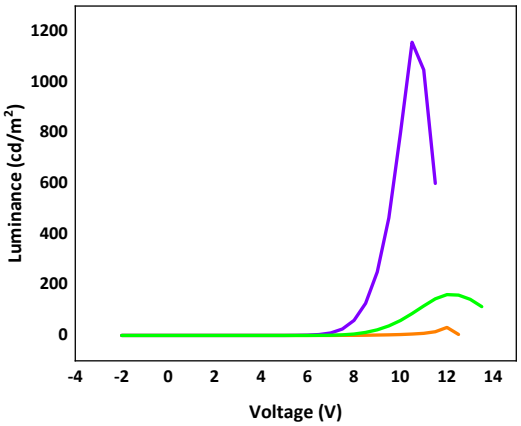

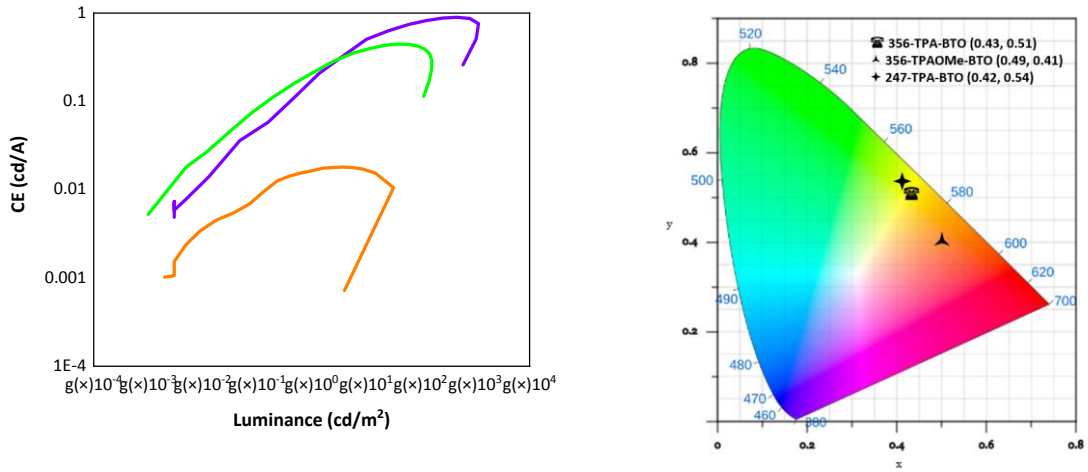

Figure 5: Current density versus voltage, (b) luminance versus voltage, and (c) current efficiency versus luminance of the best OLEDs. d) CIE chromaticity diagram 1931 of **356-TPAOMe-BTO**, **356-TPA-BTO** and **247-TPA-BTO** determined from the emission of the OLED devices. Device architecture: Glass/ITO/ PEDOT:PSS/PVK/BTO/PFN/Ag.

Table 4: Device metrics including **356-TPAOMe-BTO**, **356-TPA-BTO** and **247-TPA-BTO**

Compound	**356-TPA OMe-BTO**[a]	**356-TPA-BTO**[a]	**247-TPA-BTO**[a]	**247-TPA-BTO**[b]
$V_{turn-on}$	8.5	7.0	6.0	8.5
L_{max}(cd/m^2)	31.8	161.4	1157	19.2
CE_{max} (cd/A)	0.018	0.45	0.89	0.07
PE_{max} (lm/W)	0.006	0.151	0.306	0.02

[a] OLED fabricated on glass. [b] OLED fabricated by slot-die printing.

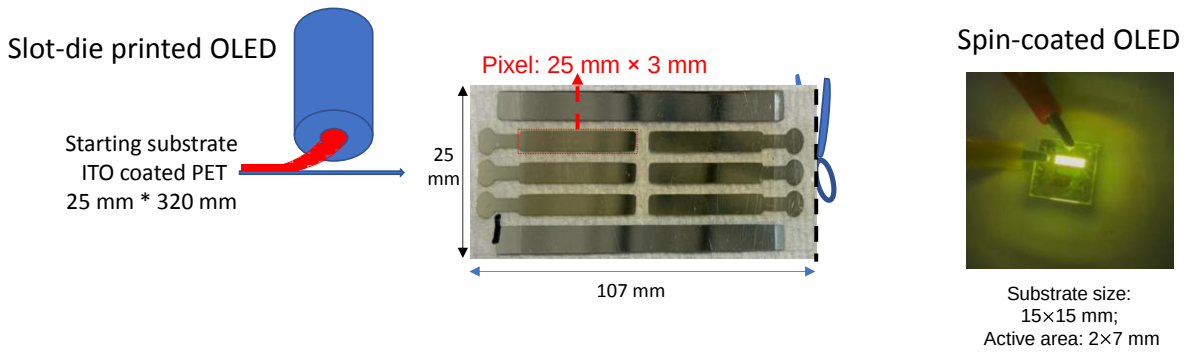

Figure 6: Pictures of slot-die printed OLED and spin coated OLED

The **247-TPA-BTO** exhibits the best characteristics on glass substrate. A voltage of 6 V can turn on the device with a maximum luminance of 1157 cd/m^2, which is quite decent for an OLED. The other compounds demonstrated that they could be turned on. Considering solubility, **356-TPA-OMe-BTO** seemed to be the most suitable compound, but **247-TPA-BTO** has the best quantum efficiency in the solid phase. It's difficult to say why one performed better than the other. **247-TPA-BTO** was selected to be applied on much larger surfaces. Following the deposition conditions on glass, this compound was deposited on PET with an ITO layer on an area of 25mm x 32 cm. All the layers have been printed via a slot-die, then the PET substrate was divided in three parts on which silver was

evaporated under vacuum using a mask to afford an active area of 75 mm^2. The resulting OLED is flexible. It could be turned on (see table 4); however, the obtained results will require optimization work since the luminance has decreased and the voltage required to turn on the OLED is higher.

Conclusion:

This article illustrates the facile synthesis of substituted S,S-dioxide benzothiophenes in positions 3, 5, and 6, as well as 2, 4, and 7. The optoelectronic characteristics reveal that the emission properties of these compounds are influenced by the oxidation state of sulfur and the regiochemistry of substitution with TPA. In the sulfone form, the compounds exhibit yellow and orange emissions, while in the sulfide form, the emission is blue. Substituting the positions in 2, 4, and 7 significantly stabilizes the LUMO+1 level, resulting in altered absorption and emission properties compared to the isomer at 3, 5, and 6, and compared to similar BTO substituted only in positions 2 and 3 as described by Tang, and in position 3 as described by Liou. OLEDs with all layers deposited through spin coating, excluding the silver layer, were successfully fabricated, exhibiting proper luminances with turn-on starting at 6V. For **247-TPA-BTO**, the research has transitioned to larger area OLEDs produced via slot-die printing. Further optimizations will be necessary to enhance performances of large area OLED.

1. Tang, C. W.; VanSlyke, S. A., Organic electroluminescent diodes. *Applied Physics Letters* **1987,** *51* (12), 913-915.
2. Tsutsui, T.; Takada, N., Progress in Emission Efficiency of Organic Light-Emitting Diodes: Basic Understanding and Its Technical Application. *Japanese Journal of Applied Physics* **2013,** *52* (11R), 110001.
3. Hong, G.; Gan, X.; Leonhardt, C.; Zhang, Z.; Seibert, J.; Busch, J. M.; Bräse, S., A Brief History of OLEDs—Emitter Development and Industry Milestones. *Advanced Materials* **2021,** *33* (9), 2005630.
4. Lochner, C. M.; Khan, Y.; Pierre, A.; Arias, A. C., All-organic optoelectronic sensor for pulse oximetry. *Nature Communications* **2014,** *5* (1), 5745.
5. Bhide, A.; Ganguly, A.; Parupudi, T.; Ramasamy, M.; Muthukumar, S.; Prasad, S., Next-Generation Continuous Metabolite Sensing toward Emerging Sensor Needs. *ACS Omega* **2021,** *6* (9), 6031-6040.
6. Jeon, Y.; Choi, H.-R.; Lim, M.; Choi, S.; Kim, H.; Kwon, J. H.; Park, K.-C.; Choi, K. C., A Wearable Photobiomodulation Patch Using a Flexible Red-Wavelength OLED and Its In Vitro Differential Cell Proliferation Effects. *Advanced Materials Technologies* **2018,** *3* (5), 1700391.
7. Murawski, C.; Gather, M. C., Emerging Biomedical Applications of Organic Light-Emitting Diodes. *Advanced Optical Materials* **2021,** *9* (14), 2100269.
8. Jou, J.-H.; Sahoo, S.; Dubey, D. K.; Yadav, R. A. K.; Swayamprabha, S. S.; Chavhan, S. D., Molecule-based monochromatic and polychromatic OLEDs with wet-process feasibility. *Journal of Materials Chemistry C* **2018,** *6* (43), 11492-11518.
9. Aizawa, N.; Pu, Y.-J.; Watanabe, M.; Chiba, T.; Ideta, K.; Toyota, N.; Igarashi, M.; Suzuri, Y.; Sasabe, H.; Kido, J., Solution-processed multilayer small-molecule light-emitting devices with high-efficiency white-light emission. *Nature Communications* **2014,** *5* (1), 5756.
10. Murat, Y.; Petersons, K.; Lanka, D.; Lindvold, L.; Yde, L.; Stensborg, J.; Gerken, M., All solution-processed ITO free flexible organic light-emitting diodes. *Materials Advances* **2020,** *1* (8), 2755-2762.
11. Rahmati, M.; Dayneko, S. V.; Pahlevani, M.; Welch, G. C., Interlayer Engineering of Flexible and Large-Area Red Organic-Light-Emitting Diodes Based on an N-Annulated Perylene Diimide Dimer. *ACS Applied Electronic Materials* **2020,** *2* (1), 48-55.
12. C, A.; Dubey, D. K.; Pahlevani, M.; Welch, G. C., Slot-Die Coating of All Organic/Polymer Layers for Large-Area Flexible OLEDs: Improved Device Performance with Interlayer Modification. *Advanced Materials Technologies* **2021,** *6* (9), 2100264.

13. Guo, J.; Hu, S.; Luo, W.; Hu, R.; Qin, A.; Zhao, Z.; Tang, B. Z., A novel aggregation-induced emission platform from 2,3-diphenylbenzo[b]thiophene S,S-dioxide. *Chemical Communications* **2017,** *53* (9), 1463-1466.
14. Zhen, S.; Guo, J.; Luo, W.; Qin, A.; Zhao, Z.; Tang, B. Z., Synthesis, structure, photoluminescence and photochromism of phosphindole oxide and benzo[b]thiophene S,S-dioxide derivatives. *Journal of Photochemistry and Photobiology A: Chemistry* **2018,** *355*, 274-282.
15. Lin, H.-T.; Huang, C.-L.; Liou, G.-S., Design, Synthesis, and Electrofluorochromism of New Triphenylamine Derivatives with AIE-Active Pendent Groups. *ACS Applied Materials & Interfaces* **2019,** *11* (12), 11684-11690.
16. Zhang, X.; Lu, Y.; Wang, H.; Chen, M.; Lin, S.; Huang, X., Palladium-Catalyzed C2-Selective Direct Arylation of Benzo[b]thiophene 1,1-Dioxides with Arylboronic Acids. *ACS Omega* **2024,** *9* (1), 1738-1747.
17. Yang, B.; Lu, Y.; Duan, L.; Ma, X.; Xia, Y.; Huang, X., Palladium-Catalyzed C2-Selective Oxidative Olefination of Benzo[b]thiophene 1,1-Dioxides with Styrenes and Acrylates. *ACS Omega* **2023,** *8* (11), 10100-10110.
18. Nakayama, J.; Sugihara, Y. J. C., Chemistry of Thiophene 1,1-Dioxides. **1999,** *31*, 131-195.
19. Thies, T., Thiophene S-Oxides. In *Chalcogen Chemistry*, Peter Papoh, N., Ed. IntechOpen: Rijeka, 2018; p Ch. 4.
20. Bailey, D.; Williams, V. E., An efficient synthesis of substituted anthraquinones and naphthoquinones. *Tetrahedron Letters* **2004,** *45* (12), 2511-2513.
21. Xia, D.; Wang, X.-Y.; Guo, X.; Baumgarten, M.; Li, M.; Müllen, K., Fused Bis-Benzothiadiazoles as Electron Acceptors. *Crystal Growth & Design* **2016,** *16* (12), 7124-7129.
22. Youssef, K.; Allain, M.; Cauchy, T.; Gohier, F., Dimerization reactions with oxidized brominated thiophenes. *New Journal of Chemistry* **2023,** *47* (15), 7375-7380.
23. Gogte, V. N.; Palkar, V. S.; Tilak, B. D., Synthesis of condensed thiophenes, diaryls and dialkyls through aryllithium and alkyllithium derivatives. *Tetrahedron Letters* **1960,** *1* (27), 30-34.
24. Daniher, F. A.; Hackley, B. E., Jr., Deoxygenation of Pyridine N-Oxides with Sulfur Dioxide. *The Journal of Organic Chemistry* **1966,** *31* (12), 4267-4268.
25. Zou, L.; Guo, S.; Lv, H.; Chen, F.; Wei, L.; Gong, Y.; Liu, Y.; Wei, C., Molecular design for organic luminogens with efficient emission in solution and solid-state. *Dyes and Pigments* **2022,** *198*, 109958.
26. Hasabeldaim, E. H. H.; Swart, H. C.; Kroon, R. E., Luminescence and stability of Tb doped CaF2 nanoparticles. *RSC Advances* **2023,** *13* (8), 5353-5366.
27. Gasonoo, A.; Beaumont, C.; Hoff, A.; Xu, C.; Egberts, P.; Pahlevani, M.; Leclerc, M.; Welch, G. C., Water-Processable Self-Doped Hole-Injection Layer for Large-Area, Air-Processed, Slot-Die-Coated Flexible Organic Light-Emitting Diodes. *Chemistry of Materials* **2023,** *35* (21), 9102-9110.